Three-dimensional numerical modelling of curved open channel using nonhydrostatic turbulent finite element solver for free-surface flows

Célestin Leupi[a,*], Edie Miglio[b], Mustafa S. Altinakar[c]

[a] *ISE-STI-LIN, Ecole Polytechnique Fédérale de Lausanne, Lausanne 1015, Switzerland*
[b] *Politecnico di Milano, Dipartimento di Matematica 'F. Brioschi', Piazza Leonardo da Vinci 32, 20133 Milano, Italy*
[c] *NCCHE, The University of Mississipi, Carrier Hall Room 102 University, MS 38677, USA*

Abstract

A novel three-dimensional model for a free-surface without the conventional hydrostatic pressure assumption has been applied to simulate the curved channel flows. Using the unstructured grid the finite element solver adopts the so-called Raviart-Thomas finite element in the horizontal plane and the conventional linear galerkin finite element in the vertical direction. The fixed strata system is used in the vertical plane and this procedure allows accurate grid resolution at the bed and the free-surface. A time-marching scheme is achieved by using the fractional three-step semi-implicit method while the characteristic method is used for the computation of convective terms. A new algorithm is used for the $k-\epsilon$ turbulence solver, and the related algebraic eddy coefficients are modified to account for some anisotropic and the related secondary effects appearing in the curved open channels flows. The model is applied successfully to the three-dimensional unsteady curved open channel flow for which experimental data are available for comparison.

Keywords: Anisotropic turbulence; Curved open channel; Secondary currents; Nonhydrostatic pressure; Lagrange–Galerkin method Raviart–Thomas finite element

1. Introduction

Nowadays with the increasing computer power, three-dimensional (3D) computations have become a practical proposition and they are often used to simulate hydrodynamic flow in natural water systems. The 3D flow in a curved open channel is a subject of significant importance in large numbers of hydraulic flows. The physical phenomena characterizing such flows is important for environmental hydraulic engineering. The main flow while passing around a bend generates secondary currents and superelevation of the water surface, due to the related centrifugal and gravity forces in the 3D helicoidal flow patterns, which, subsequently, influences the flow behaviour. These secondary flows play an important role in the channel flow and for environmental study. Several researchers have applied 3D models to simulate curved channel flow, but the 3D nature of the curved channel phenomenon is still an open question. The flow fields have been simulated in curved channels with rectangular or trapezoidal cross sections by Leschziner et al. [1], De vriend [2], Galmes et al. [3], Demuren et al. [4], Shimizu et al. [5], Ye et al. [6], and Morvan et al. [7]. Using the finite volume method on the unstructured grid, Lai et al. [8] developed a 3D model to simulate the flow in a meandering channel. Three-dimensional numerical models have been used by Wu et al. [9] and Olsen [10] to study the flow structure and mass transport in a curved open channel. Most of these 3D models employed the rigid-lid concept for the free-surface treatment. Leschziner et al. [1] indicate that the rigid lid approximation introduces some errors especially in strongly curved open channel flows. Xiabo et al. [11] have used the finite element model with conformal mesh to simulate a 3D unsteady curved open channel introducing buoyant flow and heat transfer, the standard $k-\epsilon$ turbulence model and the non-hydrostatic pressure. However, the free-surface position is not tracked and the conformal mesh could perform poorly

* Corresponding author. Tel.: +41 (21) 652 2507; Fax: +41 (21) 652 3646; E-mail: Celestin.leupi@epfl.ch

Computational Fluid and Solid Mechanics 2005
K.J. Bathe (Editor)

for some complicated bathymetry. Linear models with the hydrostatic pressure (i.e. quasi-3D or other depth-integrated flow models), and the standard $k-\epsilon$ model based on an isotropic eddy viscosity assumption, appear to be deficient in predicting complex turbulent flow for moderately and strongly curved flows.

Leupi et al. [12] proposed a novel approach based on the finite element conservative formulation using the fixed strata system for providing an accurate resolution at the bed and the free-surface. This work aims to apply a new model to simulate the curved open channel without the limitations of the hydrostatic pressure limitation and isotropic turbulence linear $k-\epsilon$ model.

In this study, the free-surface movement relies on the integrated continuity equation. The full 3D governing equations are solved by using an implicit time marching scheme. The velocity correction method has been applied to solve non-hydrostatic pressure (which is included in the momentum equations for incorporation in the surface elevation) and enforce the (local) mass conservation. Provisional velocity is solved first without the pressure term. The final velocity is obtained by combining the provisional velocity and the pressure term. Finally, the Euler or Runge-Kutta scheme is used to obtain a set of algebraic equations from discretization, and the system of equations using an implicit fractional step method (the YOSIDA scheme). An efficient fractional step algorithm from the algorithm of Mohammadi et al. [13] is introduced for the $k-\epsilon$ model. The related modified algebraic eddy viscosity expressions accounts for some anisotropic influences caused by the streamline curvature effects in the horizontal plane (see procedure of Leschziner et al. [14] and the damping effects of the free-surface and solid walls in the vertical direction [15]. The model is applied to the curved open channel 3D flows for which experimental data are available.

2. Governing equations

Consider an incompressible fluid body $\hat{\Omega}$ in a three-dimensional time-varying domain bounded by the free-surface Γ_s given by $z=\eta(x, y, t)$, where $\eta(x, y, t)$ represents the elevation of the free-surface with respect to the horizontal reference plane xy. The bottom topography Γ_b, is given by $z=-h(x, y)$, where $h(x, y)$ is the distance between the bottom and the horizontal reference plane xy such that the total water depth at the generic (x, y) coordinates point at time t is given by

$$H(x,y,t)=h(x,y)+\eta(x,y,t)$$

The turbulent fluid motion in the (x, y, z) Cartesian coordinates system is described by the Reynolds-Averaged Navier–Stokes Equations (RANS). Here the pressure p can be writen as the sum of a hydrostatic term p_h and a hydrodynamic correction $p_d = \rho q_d$ such that:

$$p(\mathbf{x},t)=p_h+p_d=p_a+g\rho_o(\eta-z)+g\int_z^{\eta}\Delta\rho\mathrm{d}z+\rho q_d(\mathbf{x},t) \tag{1}$$

The related 3D nonhydrostatic system reads:

$$\nabla_{xy}\cdot\mathbf{U}+\frac{\partial w}{\partial z}=0 \tag{2}$$

$$\frac{D\mathbf{U}}{Dt}+g\nabla_{xy}\eta-\nabla_{xy}(\nu_h\nabla_{xy}\mathbf{U})-\frac{\partial}{\partial z}\left(\nu_v\frac{\partial\mathbf{U}}{\partial z}\right)+g\nabla\left(\int_{-h}^{\eta}\frac{\Delta\rho}{\rho_o}\mathrm{d}z\right)+\nabla q_d=\boldsymbol{\lambda}_{xy} \tag{3}$$

$$\frac{Dw}{Dt}-\nabla_{xy}(\nu_h\nabla_{xy}w)-\frac{\partial}{\partial z}\left(\nu_v\frac{\partial w}{\partial z}\right)+\frac{\partial q_d}{\partial z}=0 \tag{4}$$

$$\frac{\partial\eta}{\partial t}+\nabla_{xy}\cdot\int_{-h}^{\eta}\mathbf{U}\mathrm{d}z=0 \tag{5}$$

where $\mathbf{U}=(u, v)^T$ is the horizontal velocity vector, $\boldsymbol{\lambda}_{xy}=(\lambda u, -\lambda v)^T$ is the vector of body forces with λ the Coriolis parameter, g is the gravitational acceleration, ν_h and ν_v are respectively the horizontal and vertical turbulent viscosities [16], $\nabla\cdot$ is the 3D divergence operator, D/Dt represents the material derivative, and $\nabla_{xy}\cdot$ is the surface divergence operator. ρ, ρ_0 are the fluid density and the water density, respectively.

The quantities k and ε are described by a generic form of equations [16,17]:

$$\frac{Dk}{Dt}-\nabla\cdot\left[c_\mu\frac{k^2}{\varepsilon}\nabla k\right]=c_\mu\frac{k^2}{\varepsilon}G-\varepsilon \tag{6}$$

$$\frac{D\varepsilon}{Dt}-\nabla\cdot\left[c_\varepsilon\frac{k^2}{\varepsilon}\nabla\varepsilon\right]=\frac{c_1}{2}kG-c_2\frac{\varepsilon^2}{k} \tag{7}$$

The turbulent constants' values are $c_1=0.126$, $c_2=0.07$, $c_\mu=0.09$, $c_\epsilon=1.92$.

The production term G is represented by the squared shear [8]

$$G=\frac{1}{2}\left(\|\nabla\mathbf{V}\|+\|\nabla\mathbf{V}\|^T\right)^2 \tag{8}$$

where $\|\cdot\|$ represents the Euclidian norm and $\mathbf{V}$ is the three-dimensional velocity field. Integrating the continuity equation in the z direction and using the suitable kinematic boundary conditions at the bottom and the free-surface, we obtain Eq. (5), which describes the evolution of the free-surface. The suitable boundary conditions are implemented and the standard wall functions are applied to the bed according to the roughness coefficient [9,12].

In Eq. (3), the turbulent viscosities are

$$\nu_t = c_\mu \frac{k^2}{\varepsilon}; \qquad \nu_v = \gamma_v \nu_t; \qquad \nu_h = \gamma_v \nu_t \tag{9}$$

in which ν_t is the isotropic turbulent viscosity calculated by the standard $k-\epsilon$ model. The streamline curvature effect γ_h derived by Leschziner et al. [14] is expressed as

$$\gamma_h = \frac{1}{1 + 0.57 \frac{k^2}{\varepsilon^2}\left(\frac{\partial V_s}{\partial n} + \frac{V_s}{R}\right)\frac{V_s}{R}} \tag{10}$$

The influence of the free-surface and the bottom, derived by Naot et al. [15], is expressed as

$$\gamma_v = \frac{C_v^2}{(C_v + 0.15\alpha_2)\,(C_v + 0.2\alpha_2)} \tag{11}$$

and

$$C_v = 1.5 - 0.5\alpha_1; \quad \alpha_1 = \left(\frac{L}{z_1}\right)^2; \quad \alpha_2 = \left(\frac{L}{z_2}\right)^2; \quad z_1 = \left\langle \frac{1}{z} \right\rangle^{-1/2} \tag{12}$$

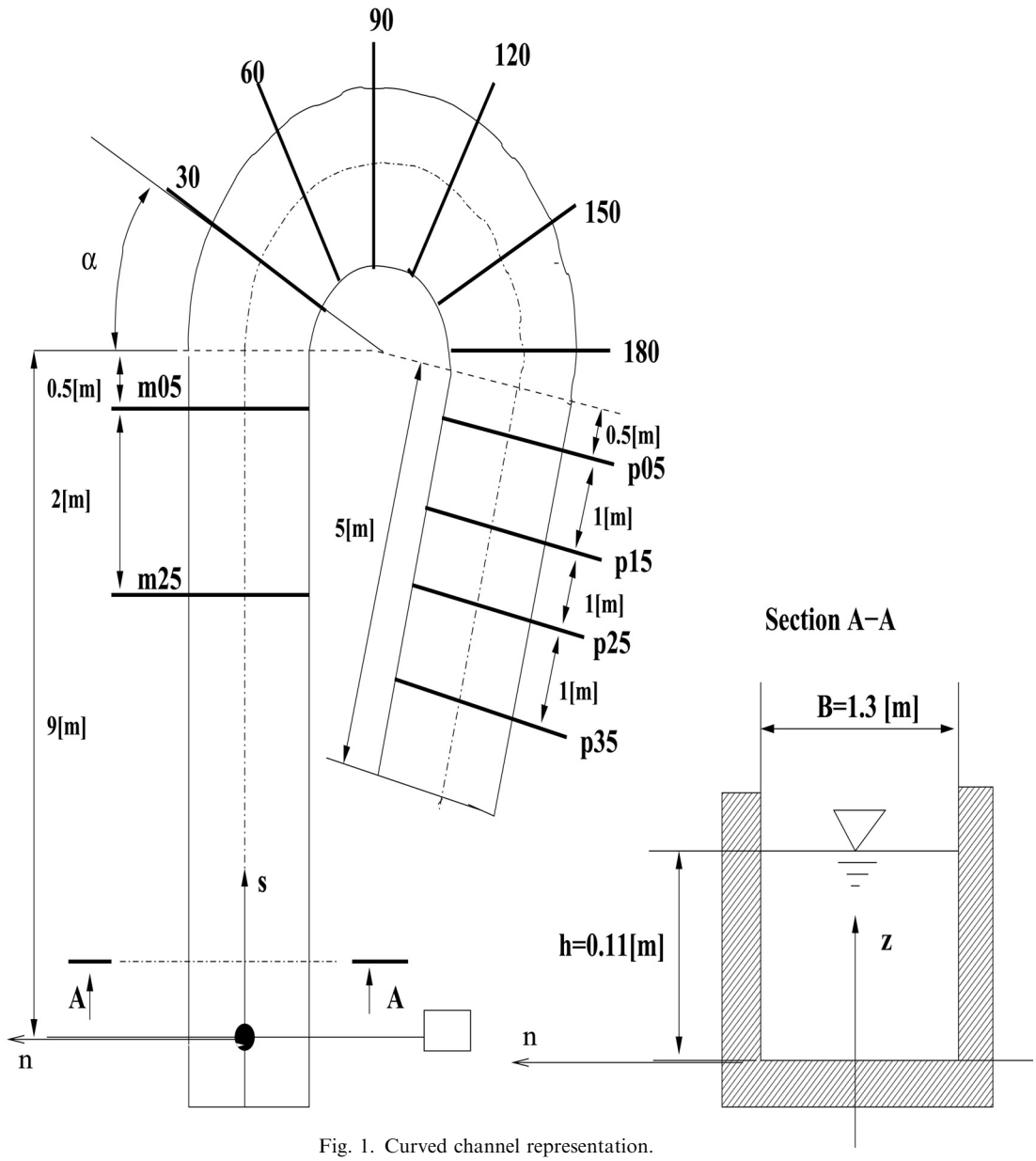

Fig. 1. Curved channel representation.

$$z_2 = \left\langle \frac{1}{(H-z)^2} \right\rangle^{-1/2} + 0.31662L; \quad L = \left(\frac{C_\mu^{3/4}}{k} \right) \frac{k^{3/2}}{\varepsilon} \tag{13}$$

where V_s = downstream velocity component, R = local radius of curvature of streamline, n = normal distance from the wall, L = dissipation length, and z_1, z_2 = root-mean-squared reciprocal distances from the solid walls and free-surface respectively.

To obtain a stable turbulence scheme and preserve positivity of k and ϵ, the set of convection-diffusion equations are solved using a fractional step scheme [13], which relies on the splitting of a convection step and a diffusion step [12,19].

For the overall time-discretization method, the convection terms are discretized using the characteristics method (Lagrange–Galerkin), by using either a Euler scheme or the more accurate Runge-Kutta algorithm. The vertical diffusion terms in the advection-diffusion

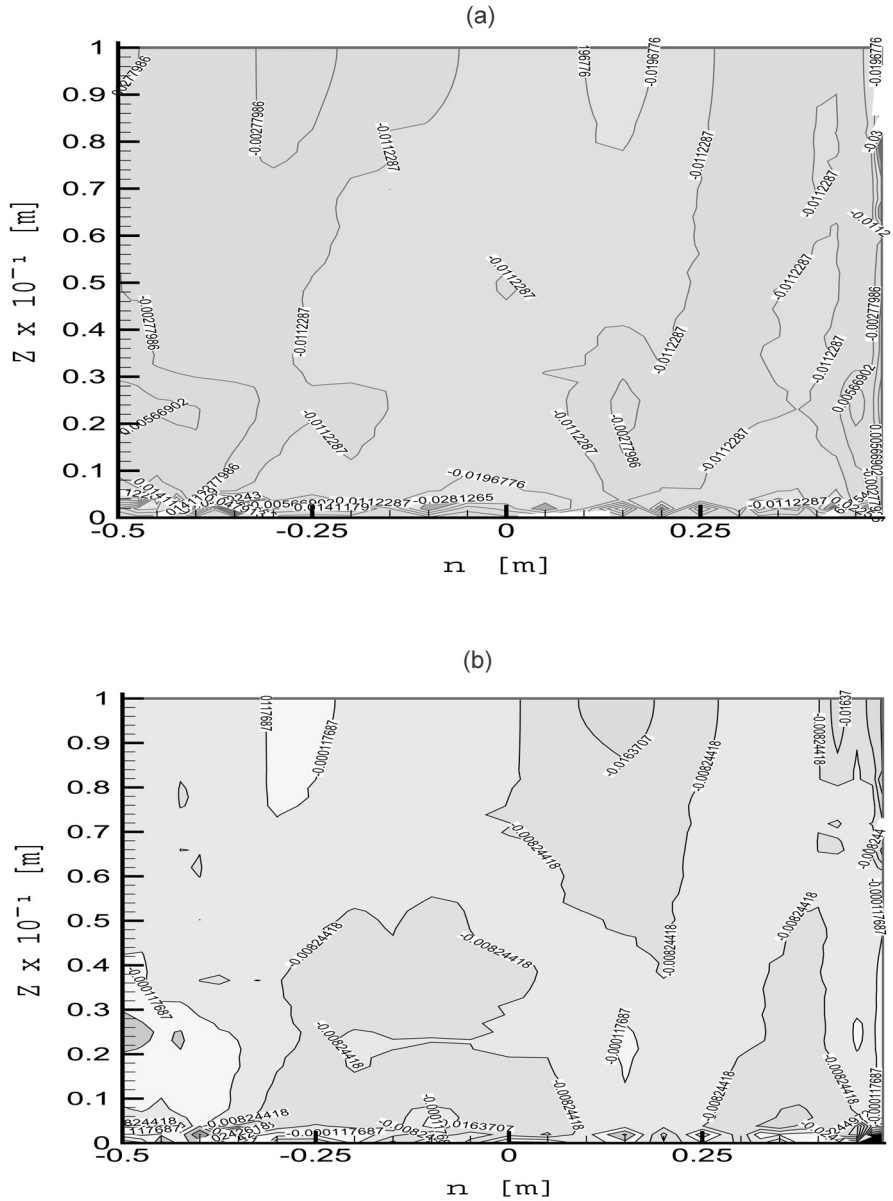

Fig. 2. Isocontours of the transversal velocity component V_n of cross-stream at the section m05: (a) measured; (b) nonhydrostatic solution.

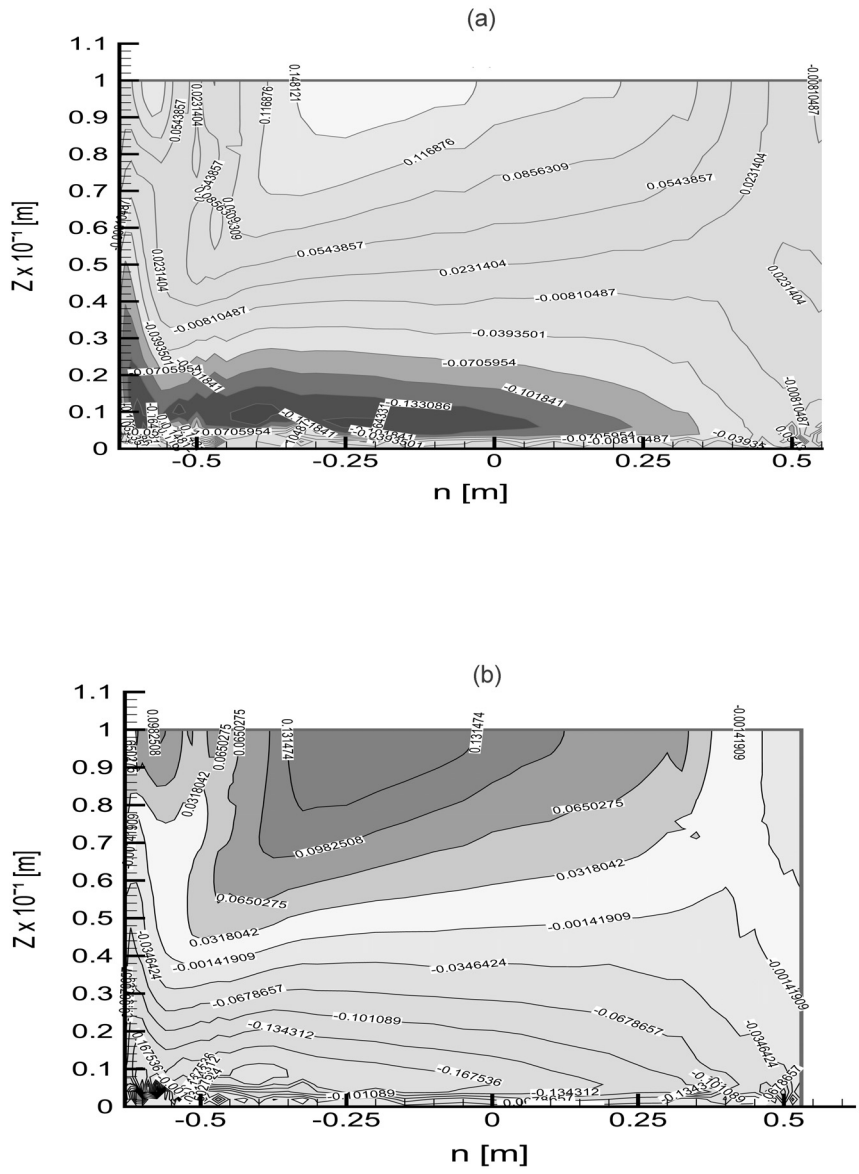

Fig. 3. Isocontours of the transversal velocity component V_n of cross-stream at the section $\alpha = 90$: (a) measured; (b) nonhydrostatic solution.

equation are discretized implicitly. The source terms are discretitized explicitly, while the sink terms are discretized using the quasi-implicit form. At each time step the algebraic system is solved using the conjugate gradient solver.

3. Numerical results

Detailed experimental data for testing the solver are limited. However, the unsteady flow in the curved open channel is a suitable test case for the numerical scheme, as experimental data are provided in the thesis of Blanckaert [20] at the Laboratoire d'Hydraulique Environnementale (LRH) of the Swiss Federal Institute in Lausanne. The channel layout and dimensions are shown in Fig. 1. The discharge is set to $Q = 0.089$ [m/s] with the flat bed, the rough bed height is $k_s = 0.001$ [m]. The flow depth at the outflow (donwstream end of the flume) is 0.159 [m]. The computational grid is composed of 50.000 elements and 30.000 nodes and the time step is set to 0.1 [s]. Figures 2, 3, and 4 show the isocontours of the experimental measurements and computed solutions

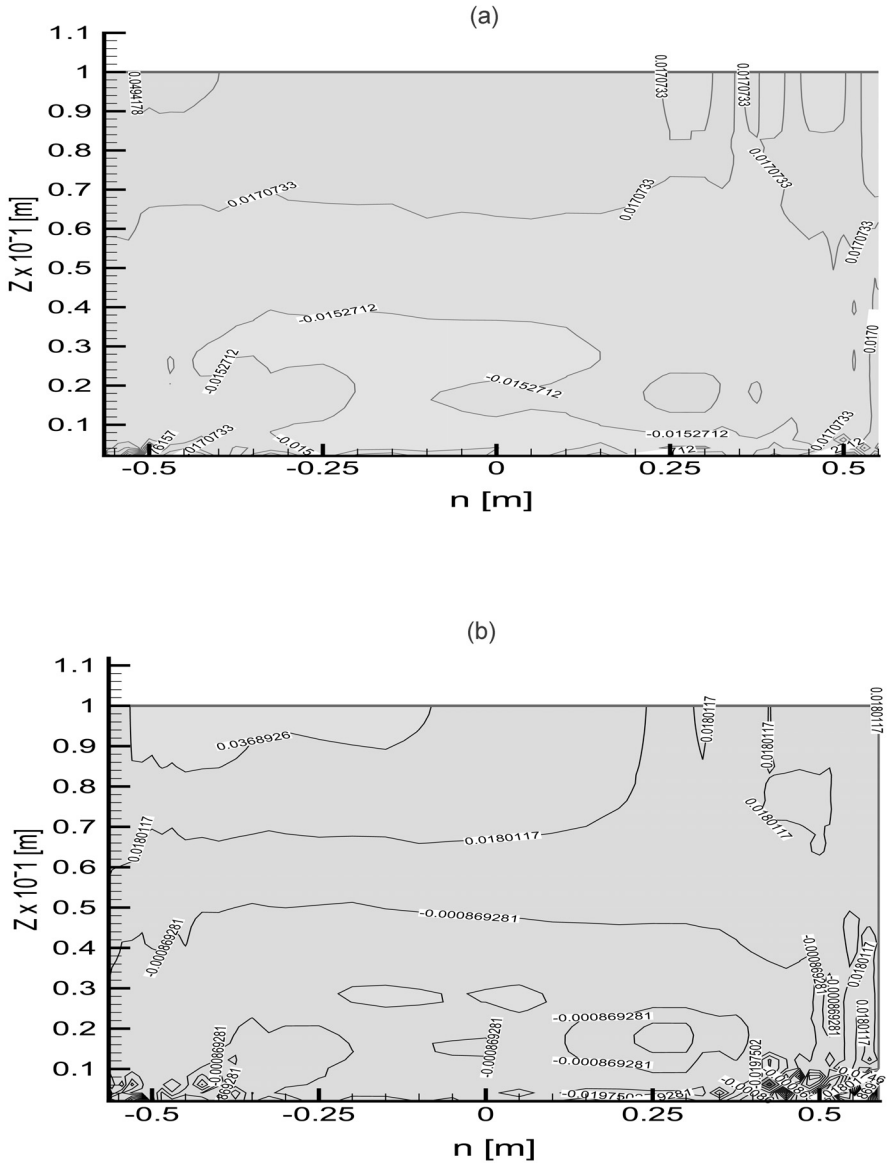

Fig. 4. Isocontours of the transversal velocity component V_n of cross-stream at the section p25: (a) measured; (b) nonhydrostatic solution.

of the transverse velocity component in cross-sections at the selected sections, respectively. From data analysis, the role of the advection momentum transport by the cross-stream circulation on the distribution of downstream velocity and bottom shear stress is more important [20]. The water elevation at the outer bank is normally higher than that at the inner bank. The balance of the non-uniform centrifugal force and the non-uniform inward pressure gradient pushes the upper part of the flow towards the outer bank and the lower part of the flow towards the inner bank. This flow is superimposed on the main flow and results in helical flow over the entire reach of the curved channel.

Some features and processes underlying the full 3D flow can also be observed from computation. Using the Lagrange–Galerkin method for the advection terms and including the non-hydrostatic pressure in the momentum equations for incorporation in the surface elevation (for providing the local continuity) leads to the accurately dynamical description of the cross-stream circulation effects of the fluid flow. The incorporation of the free-surface movement instead of the rigid-lid

approximation, the use of non-hydrostatic pressure and the modified eddy viscosity accounts for a wave-like oscillation of the pattern of circulation cells embedded in background anisotropic turbulence.

In the inward straight part of the channel (see Fig. 2), only one major secondary flow eddy is observed (probably due to the fact that, in this region, such a mechanism relies strongly on the anisotropy of turbulence). In the curved part, the outer bank cells rely on both turbulence anisotropy and the critical value of the curvature. In fact, besides the classical helical motion, a weaker and smaller outer bank is well observed near the outer bank in the curvature (see Fig. 3). The outward region (Fig. 4) is reproduced successfully. The adoption of the multi-layers in the vertical direction allow a higher mesh density near the free-surface and the bottom, leading to an improvement in the solutions.

4. Conclusion

In this work we proposed a semi-implicit non-hydrostatic 3D multi-layer hybrid finite element model including the robust fractional step for the $k-\epsilon$ solver. The model used the Lagrange–Galerkin approach for the advection terms and the eddy coefficients, modified to account for some anisotropic effects appearing in open curved channels. More insight has been obtained in the processes underlying the interesting features of the flow field such as multi-cellular pattern of the secondary circulation due probably to the curvature influence on the turbulence.

The model describes accurately the effect of cross-stream circulation and related secondary effects, by means of the modified eddy coefficients obtained from the linear $k-\epsilon$ turbulence closure and full 3D finite elements with non-hydrostatic pressure considerations.

The tests were performed in order to validate the model against well-known flow cases. Compared to the experimental measurements, the computed solutions perform well and reproduce successfully the secondary circulations.

Acknowledgment

The first author gratefully acknowledges funding from SWISS National Science Foundation through grant number 21–65095.01. Michel Deville and Alfio Quarteroni are acknowledged for their fruitful discussions.

References

[1] Leschziner MA and Rodi W. Calculation of strongly curved open channel flow. ASCE J Hydr Div 1979; 103(10):1297–1314.

[2] De vriend HJ. Velocity redistribution in curved rectangle channel flow. J Fluid Mech 1981;107(6):423–439.

[3] Galmes JM and Lakshminarayana B. Turbulence modeling of three-dimensional shear flows over curved rotating bodies. AIAA J 1984;22(10):1420–1428.

[4] Demuren AO, Rodi W. Calculation of flow and pollutant dispersion in meandering channels. J Fluid Mech 1986;172(11):65–92.

[5] Shimizu Y, Yamaguchi Y and Itukara T. Three-dimensional computation of flow and bed deformation. ASCE J Hydr Eng 1990;116(9):1090–1107.

[6] Ye J and McCorquodale JA. A 3D free surface hydrodynamic modelling with curviligne coordinate collocated grid arrangement. Rep No 1996–01, Great Lakes Institute for Environmental Research, University of Winsor, Canada, 1996.

[7] Morvan H, Pender G, Wright NG and Ervine DA. Three-dimensional hydrodynamics of meandering compound channels. ASCE J Hydr Eng 2002;128(7):674–682.

[8] Lai YG, Weber LJ and Patel VC. Three-dimensional model for hydraulic flow simulation. I: formulation and verification. ASCE J Hydr Eng 2003;129(3):196–205.

[9] Wu W, Rodi W, and Wenka T. 3D numerical modeling of flow and sediment transport in open channels. ASCE J Hydr Eng 2000;126(1):4–15.

[10] Olsen NRB. Three-dimensional CFD modeling of self-forming meandering channel. ASCE J Hydr Eng 2003;129(5):366–372.

[11] Chao X, Jia Y and Wang SSY. Three-dimensional simulation of buoyant heat transfer in a curved open channel. In: Proc International Conference on Advances in Hydroscience and Engineering, ICHE, NCCHE Mississipi, USA, 2004;6:18–19.

[12] Célestin Leupi, Edie Miglio, Mustafa Altinakar, Alfio Quarteroni and Michel Deville. QUASI-3D Finite element shallow-water flow with $k-\epsilon$ turbulence Model. In: Proc International Conference on Advances in Hydro-science and Engineeering, ICHE, NCCHE Mississipi, USA, 2004;6:400.

[13] Mohammadi B, Pironneau O. Analysis of k – epsilon turbulence model. Chichester: J Wiley & Sons, 1994.

[14] Leschziner MA, Rodi W. Calculation of annular and twin parallel jets usng various discretization schemes and turbulence-model variations. ASCE J Fluids Eng 1981;103(2):352–360.

[15] Naot D, Rodi W. Numerical simulation of secondary currents in channel flow. ASCE J Hydr Div 1982;108(8):948–968.

[16] Rodi W. Turbulence Models and their Application, 2nd edn. Delft, The Netherlands: International Association for Hydraulic Research, 1984.

[17] Launder BE, Spalding DB. The numerical computation of turbulent flows. Comput Methods Appl Mech Eng 1974;3:269–289.

[18] Luyten PJ, Jones JE, Proctor R, Tabor A, Tett P, Wild-Allen K. COHERENS: a coupled hydrodynamical–ecological model for regional and shelf seas: user documentation. MUMM report, Management Unit of the Mathematical Models of North Sea, 914pp.

[19] Leupi C, Miglio E, Altinakar M, Quarteroni A and

Deville M. 3D finite element solver for shallow-water flow with $k - \epsilon$ turbulence model. ASCE J Hydr En. (submitted).

[20] Blanckaert K. Flow and turbulence in sharp open-channel bends. PhD thesis no. 2545, EPFL, Lausanne, Switzerland, 2002.